

Article

# Fatigue Damage Evaluation of Compressor Blade Based on Nonlinear Ultrasonic Nondestructive Testing

Pengfei Wang <sup>1,2,\*</sup> , Weiqiang Wang <sup>3</sup>, Sanlong Zheng <sup>1,2</sup>, Bingbing Chen <sup>1,2</sup> and Zengliang Gao <sup>1,2</sup>

<sup>1</sup> Institute of Process Equipment and Control Engineering, College of Mechanical Engineering, Zhejiang University of Technology, Hangzhou 310023, China; slzheng2020@163.com (S.Z.); bingbingchen2020@163.com (B.C.); zenglianggao2020@163.com (Z.G.)

<sup>2</sup> Engineering Research Center of Process Equipment and Re-Manufacturing, Ministry of Education, Zhejiang University of Technology, Hangzhou 310023, China

<sup>3</sup> School of Mechanical Engineering, Shandong University, Jinan 250012, China; wqwang59@163.com

\* Correspondence: pfwang@zjut.edu.cn

**Abstract:** Nonlinear ultrasonic testing is highly sensitive to micro-defects and can be used to detect hidden damage and defects inside materials. At present, most tests are carried out on specimens, and there are few nonlinear ultrasonic tests for fatigue damage of compressor blades. A vibration fatigue test was carried out on compressor blade steel KMN, and blade specimens with different damage degrees were obtained. Then, the nonlinear coefficients of blade specimens were obtained by nonlinear ultrasonic testing. The results showed that the nonlinear coefficient increased with the increase in the number of fatigue cycles in the early stage of fatigue, and then the nonlinear coefficient decreased. The microstructures were observed by scanning electron microscopy (SEM). It was proven that the nonlinear ultrasonic testing can be used for the detection of micro-cracks in the early stage of fatigue. Through the statistical analysis of the size of the micro-cracks inside the material, the empirical formula of the nonlinear coefficient  $\beta$  and the equivalent crack size were obtained. Combined with the  $\beta$ - $S$ - $N$  three-dimensional model, an evaluation method based on the nonlinear ultrasonic testing for the early fatigue damage of the blade was proposed.

**Keywords:** vibration fatigue; nonlinear ultrasonic; nonlinear coefficient; compressor blade; fatigue damage evaluation



**Citation:** Wang, P.; Wang, W.; Zheng, S.; Chen, B.; Gao, Z. Fatigue Damage Evaluation of Compressor Blade Based on Nonlinear Ultrasonic Nondestructive Testing. *J. Mar. Sci. Eng.* **2021**, *9*, 1358. <https://doi.org/10.3390/jmse9121358>

Academic Editors: K. Reza Kashyzadeh and Mahmoud Chizari

Received: 23 October 2021  
Accepted: 26 November 2021  
Published: 1 December 2021

**Publisher's Note:** MDPI stays neutral with regard to jurisdictional claims in published maps and institutional affiliations.



**Copyright:** © 2021 by the authors. Licensee MDPI, Basel, Switzerland. This article is an open access article distributed under the terms and conditions of the Creative Commons Attribution (CC BY) license (<https://creativecommons.org/licenses/by/4.0/>).

## 1. Introduction

Many studies have shown that a material's early performance degradation stage occupies 80%–90% of the material's fatigue life [1]. The acoustic parameters measured by the existing ultrasonic technology in the linear range generally have a relatively small response to the early damage changes of materials and structures, and the degradation of mechanical properties cannot be quantitatively characterized. Although other traditional detection methods such as penetration and radiation are widely used, they are less sensitive to small damage such as micro-defects and micro-cracks, especially the hidden damage inside the material. Recent studies have shown that nonlinear ultrasonic technology can overcome the shortcomings of linear ultrasonic techniques that are not sensitive to material or structure damage changes in the early and mid-term. The reason for this is that the nonlinear effect of ultrasonic propagation in materials is closely related to material performance degradation. That is to say, material performance degradation will cause the generation of nonlinear harmonics of ultrasonic propagation [2–5].

Nonlinear ultrasonic technology is highly sensitive to micro-defects or damage, and can be used to detect hidden damage and defects inside materials [6,7]. Nagy et al. [8] used nonlinear ultrasonic tests to evaluate the performance degradation of the material before cracks appeared and to predict the fatigue life of the material. Jhang et al. [9] studied the relationship between the deterioration of the mechanical properties of materials

and the nonlinear coefficient under tensile loading. Kawashima [10] completed the detection of non-metallic inclusions in continuum cast steel with a nonlinear scanning system. In 2011, Viswanath [11] found that nonlinear coefficients can be used to characterize the degradation of the mechanical properties of materials under tensile load. Cremer et al. [12] used nonlinear ultrasonic technology to observe the evolution of very high cycle fatigue damage of welded joints of aluminum alloy in situ. Li [13] conducted in situ observations of the very high cycle fatigue characteristics of aluminum alloys with nonlinear ultrasonic and found that the ultrasonic nonlinear coefficients are more sensitive to crack initiation and propagation. In addition, the ultrasonic nonlinear coefficient has a good correlation with the stiffness and plastic strain of the specimen. Yan [14,15] proposed a comprehensive model of dislocations that includes various factors. This model can predict the change state of nonlinear ultrasonic coefficient of metal materials in the process of fatigue damage. Feng Wei [16] used his own built-up nonlinear ultrasonic inspection system to perform multi-point fast nonlinear ultrasonic testing on fatigue damage of aluminum alloy. Li [17] carried out Rayleigh surface wave measurements on Q235 steel in different tensile damage and corrosion fatigue damage. It was found that the nonlinear ultrasonic coefficient has a monotonically increasing relationship with the number of fatigue cycles. Gao [18] found that the Lamb wave nonlinear coefficient in the aluminum plate has no obvious relationship with the change of the fundamental frequency signal amplitude, but the double-frequency signal wave amplitude increases with the number of fatigue cycles in the initial fatigue damage. Wang [19] used a nonlinear ultrasonic device to conduct studies on two aluminum alloy sheets of 6061-t6 and 5A06 and found that the different surface finishes of the test specimens will have a greater impact on the results of nonlinear ultrasonic testing. Zhang [20] conducted research on nonlinear ultrasonic testing of complete fatigue-damaged aluminum plates, fatigue-damaged aluminum plates with holes, and damaged aluminum plates repaired with composite materials. It was found that the relative second-order ultrasonic nonlinear parameters measured in the experiment were relatively consistent with the overall process of dislocation, crack generation, and propagation during fatigue damage. Bian [21] discussed the interaction between Lamb wave and through-hole damage by numerical simulation of the fluctuation process of  $A_0$  and  $S_0$  modes in Lamb wave. In addition, neural network theory was introduced in ultrasonic Lamb wave damage detection, and the degree of damage to the aluminum plate was successfully predicted.

With the increase in the speed of large centrifugal compressors and the complexity of the service environment, fatigue failure of the blade has occurred from time to time. The blade resonance caused by wake-induced vibration is the main source of its fatigue load. At this time, the load on the blade is the vibration load with one end fixed. In engineering, the detection of the micro-cracks of the blade at the early fatigue stage has become very important. Nonlinear ultrasonic testing is mainly used to characterize the damage with the second harmonic of the received signal. Linear ultrasonic testing is mainly used to measure acoustic parameters such as wave speed and attenuation. Nonlinear ultrasonic testing is more sensitive to micro-defects in the early stage of damage. At present, there are few studies on nonlinear ultrasonic testing for vibration fatigue load. Most of the fatigue tests are performed on materials, and there are few nonlinear ultrasonic detections for fatigue damage of the compressor blade. The influence of the three-dimensional structure of the blade and the surface state after service is not considered. Two sets of KMN fatigue tests were carried out in the previous work [22]. One set of specimens was subjected to bending fatigue test, and the other set was subjected to bending fatigue test with initial tensile load. Therefore, the authors performed vibration fatigue tests on KMN, a commonly used material for centrifugal compressor blades, under simulated working conditions, and performed nonlinear ultrasonic testing on specimens with different fatigue damage levels. The mapping relationship between the fatigue damage of the blade material KMN and the nonlinear coefficient was studied, and the initial fatigue damage evaluation method of the blade material based on nonlinear ultrasonic testing was proposed, which has important

theoretical guiding significance for the fatigue damage detection and the safe and reliable operation of the blade.

## 2. Materials and Methods

### 2.1. Experimental Materials

KMN steel is a low-alloy high-strength steel with a grade of 15Cr2Mo1. According to the requirements of the standard GB/T228-2010 “Metal Material Room Temperature Tensile Test Method”, a universal material testing machine was used to test the mechanical properties of the KMN material. Moreover, the density was obtained by measuring the weight difference of the test plate in air and water [23,24]. Its mechanical properties and chemical composition are shown in Tables 1 and 2, respectively. The heat treatment process of KMN steel is shown in Table 3.

**Table 1.** Mechanical properties of KMN.

Mechanical Properties	Tensile Strength $R_m$ (MPa)	Yield Strength $R_{p0.2}$ (MPa)	Elastic Modulus $E$ (GPa)	Density $\rho$ (kg/m <sup>3</sup> )	Hardness $HV$ (kgf·mm <sup>-2</sup> )
KMN	1193	1072	205	7840	335
Standard deviation	2.52	6.51	1.15	10.07	4.04

**Table 2.** Chemical composition of KMN (wt.%).

Chemical Composition	C	Mn	Si	Mo	Cr	P	S
KMN	0.13–0.18	0.5–0.8	0.17–0.37	0.9–1.1	2.2–2.5	≤0.030	≤0.030

**Table 3.** Heat treatment process of KMN.

Heat Treatment	Temperature (°C)	Holding Time (h)	Cooling Method
Quenching	970 ± 10	2.5–3	Oil cooling
Tempering	570 ± 10	4–5	Air cooling

All test plates in this paper were from Shenyang Blower Works Group Corporation. The parameters in Table 3 refer to the technical requirements of the compressor blade heat treatment [25]. The heat treatment process of KMN steel involves quenching at 980 ± 10 °C for 1–1.5 h followed by oil cooling and then tempering at 700–750 °C for 1.5–2 h before air cooling. The metallographic specimen of KMN is corroded by nitric acid alcohol. The microstructure of KMN is shown in Figure 1. The metallographic structure is mainly needle-like and lath-like martensite. The microstructure is small and the distribution is relatively uniform. Some tiny inclusions can be found in the microstructure, and the size is about 1–2 μm.

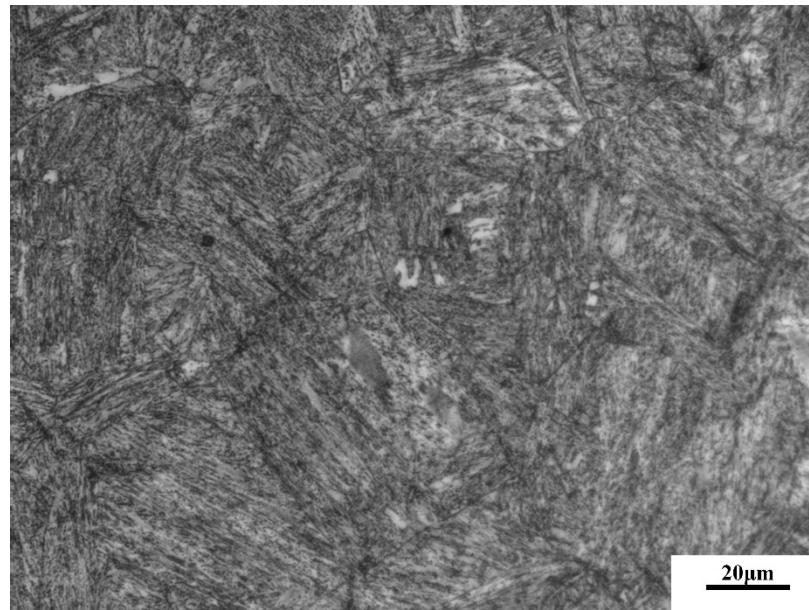


**Figure 1.** Microstructure of the KMN steel.

## 2.2. Experimental Methods

The ET-10d-240 type vibration test bench was used to perform a vibration fatigue test on the KMN specimen. The shape and size of the fatigue specimen are shown in Figure 2, and the thickness was 2 mm. The blade specimen was taken from impeller and the three-dimensional structure and the surface state after service was preserved, as shown in Figure 3. Before the fatigue test, the specimen surface was mechanically polished to keep the surface state consistent. The roughness  $R_a = 0.2$ .

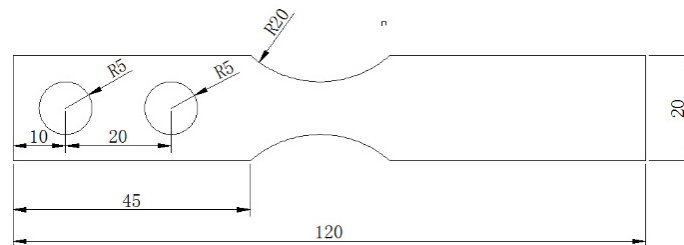


**Figure 2.** Shape and dimensions of the KMN vibration fatigue specimen (mm).

During the test, one end of the specimen was fixed on the surface of the vibration test bench by the fixture, and the other end was free to vibrate. When the excitation frequency of the vibration test bench was near the resonance frequency of the specimen, the specimen resonated. The measured first-order bending resonance frequency of the specimen was 59 Hz. The KMN specimen was subjected to fatigue loading with different cycles (until  $10^7$ ) using the vibration test bench, and fatigue specimens with different cycles were obtained, as shown in Figure 4. The acceleration control model was used during the test, the test temperature was room temperature, the loading waveform was sine wave, the loading frequency was 59 Hz, and the acceleration was  $5 \text{ m/s}^2$ . The vibration test in this paper followed HB 5277-1984 “Vibration Fatigue Test Method of Engine Blade and Material”. The main cause of blade fatigue failure was wake-induced vibration, and the first-order bending resonance frequency of the fatigue specimen was 59 Hz [25].



(a)

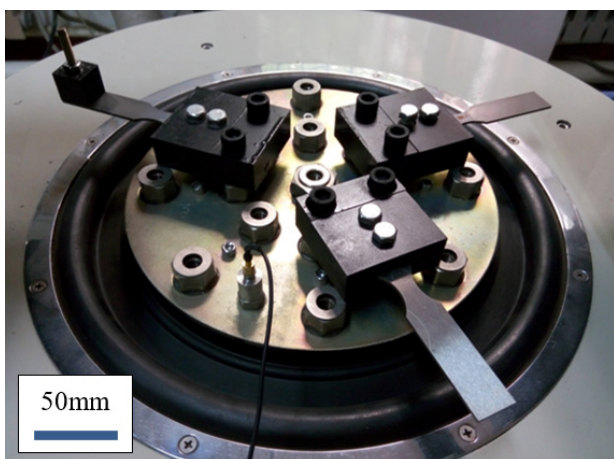


(b)

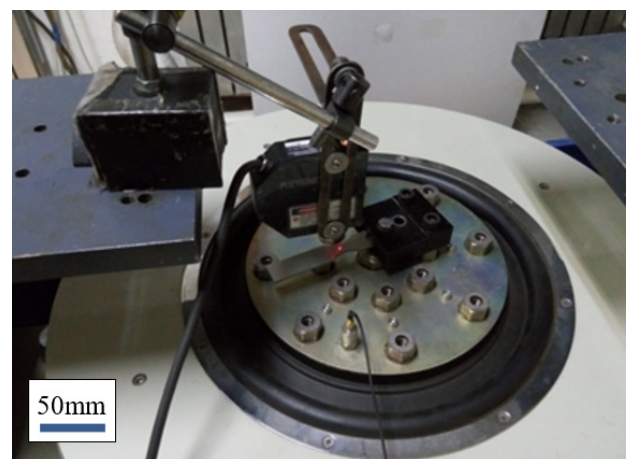


(c)

**Figure 3.** Impeller and KMN blade specimen. (a) Impeller; (b) KMN blade specimen after service; (c) top view of blade specimen.



(a)



(b)

**Figure 4.** Vibration fatigue test of KMN. (a) Vibration test bench; (b) laser displacement sensor.

The RitecSNAP high-energy ultrasonic system was used to perform ultrasonic Lamb wave nonlinear measurements on KMN specimens with different fatigue damage, as shown

in Figure 5. The pulse signal was excited by a signal generator, filtered by a low-pass filter, and then transmitted to the ultrasonic piezoelectric transducer. At this time, the voltage signal was converted into an ultrasonic vibration signal and entered the material to be measured. After wave propagation in the specimen, the ultrasonic signal was received by the piezoelectric transducer under the action of the nonlinear stress and strain of the material, and then obtained after passing through a high-pass filter. During the experiment, a narrowband piezoelectric transducer with a center frequency of 5 MHz was used as the transmitting probe, and a broad-band piezoelectric transducer with a central frequency of 10 MHz was used as the receiving probe. The frequency of the excitation signal was 5 MHz, the sampling rate of the oscilloscope was 1.25 GS/s, and the incident angle was  $27^\circ$  [22]. The probes at both ends were fixed by a fixture, and the pressure on the base surface of the probe was controlled at a relatively similar level during each measurement using a pressure sensor.

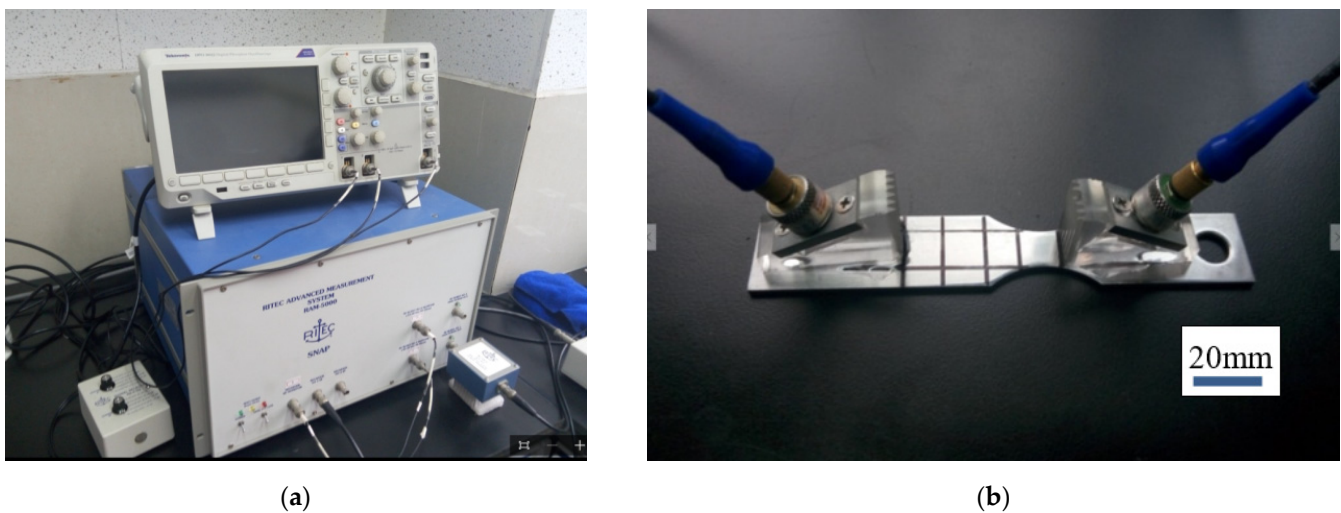


**Figure 5.** Nonlinear ultrasonic test system. (a) RitecSNAP ultrasonic system; (b) specimen and ultrasonic piezoelectric transducer.

The coupling agent was glycerin. Because the coupling layer was very thin, the nonlinearity of the coupling agent can be ignored. Secondly, in order to reduce the impact of elastic nonlinear effect of the plexiglass, the propagation distance of the longitudinal wave excited by the transducer in the wedge-shaped block was shortened as much as possible [26]. Due to the nonlinearity of the solid medium, the stress–strain relationship exhibited nonlinear characteristics.  $\beta$  is the parameter describing the degree of material nonlinearity, namely, the second-order nonlinear coefficient. According to the one-dimensional longitudinal wave nonlinear wave equation in the solid medium, the second-order nonlinear coefficient  $\beta$  can be expressed as  $\beta = \frac{8}{k^2_x} \frac{A_2}{A_1^2}$  [27–29].  $A_1$  is the amplitude of the fundamental frequency signal, and  $A_2$  is the amplitude of the second harmonic signal. The signal obtained in the experiment contained the fundamental frequency and high-order signal. These signals were processed by short-time Fourier transform (STFT). The amplitude of the fundamental frequency and the second-order frequency Lamb wave were obtained. Then, the second-order nonlinear coefficient  $\beta$  can be expressed with  $A_2/A_1^2$  [27–29].

### 3. Results

#### 3.1. Dispersion Curve

The frequency dispersion characteristics of ultrasonic guided waves caused the generation efficiency of the second harmonic to be very low in general, and the signal of the second harmonic was very weak, which is inconvenient for actual measurement. If the phase velocities of the fundamental frequency Lamb wave mode and the double frequency Lamb wave mode excited in the solid plate are equal, then the obvious Lamb

wave accumulation second harmonic signal can be measured. Therefore, we measured the dispersion curves of Lamb wave of KMN specimen [22]. In order to excite the Lamb wave second harmonic signal with the accumulation effect, we could choose to excite the fundamental frequency Lamb wave of 2.25 MHz. At this time point, the phase velocity of the fundamental frequency and the double frequency were equal.

It is necessary to measure and check the amplitude–frequency response for the experimental platforms such as the RitecSNAP system, transmitting and receiving transducers, etc. This is to determine that the measured Lamb wave second harmonic signal comes from the nonlinearity of the material being tested, rather than from the nonlinearity of the measurement system.

When the incident voltage is fixed, there is a linear relationship between  $A_2/A_1^2$  and the propagation distance. We kept the incident voltage signal unchanged and changed the distance of the two transducers (10–40 mm). From Figure 6, we can see that when the propagation distance was relatively close, as the propagation distance increased,  $A_2/A_1^2$  also increased, which shows that the second harmonic signal we received came from the specimen itself. When the propagation distance was great, the value of  $A_2/A_1^2$  decreased instead. This is mainly determined by the size and shape of the specimen. When the propagation distance increased, the coupling of the signal in the specimen became worse. Therefore, we use a propagation distance of 10 mm in the subsequent experiments. At this time, the second harmonic signal was generated by the Lamb wave propagating in the material, rather than the harmonic signal generated by the wedge-shaped block or coupling agent.

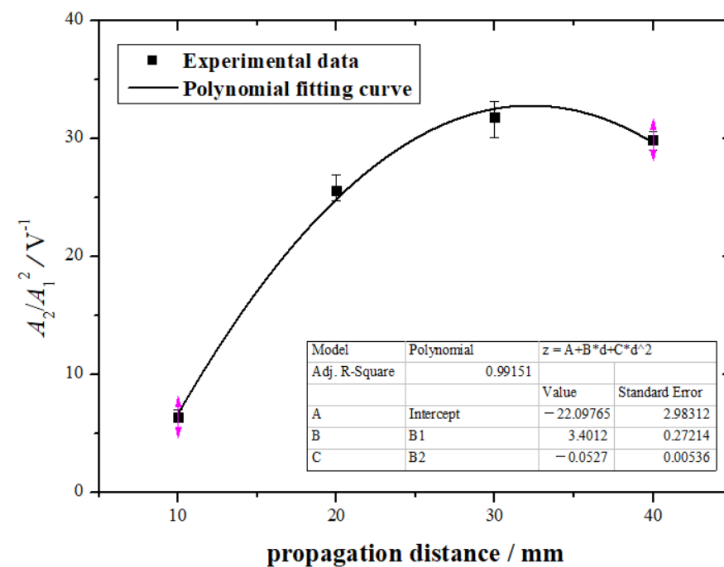


**Figure 6.** Relationship curve between  $A_2/A_1^2$  and the propagation distance of KMN vibration fatigue specimen. ( $R^2 = 0.99$ ).

### 3.2. $\beta$ -N Curve

Nonlinear ultrasonic testing was carried out on fatigue specimens and the time domain signals were obtained. The time domain signals were processed with STFT (short-time Fourier transform) and the STFT time-frequency energy spectrum image of KMN specimen was obtained. The STFT energy spectrum is represented by 256 levels of gray scale. Look up the amplitude table (the horizontal axis is the time and the vertical axis is the frequency) and the maximum amplitude of fundamental wave  $A_1$  and second harmonic wave  $A_2$  can be obtained. In this experiment, due to the complexity of the time-domain signal obtained and the overlapping of multiple waveforms, it was difficult to distinguish the signal we needed when using FFT. Therefore, our subsequent analysis used STFT for Fourier transform, which can effectively extract the  $S_1$  and  $S_2$  signals.  $A_2/A_1^2$  was used as the

normalized nonlinear coefficient to characterize the fatigue damage, and the relationship curve between the nonlinear ultrasonic coefficient  $\beta$  and the number of fatigue cycles was obtained, as shown in Figure 7.

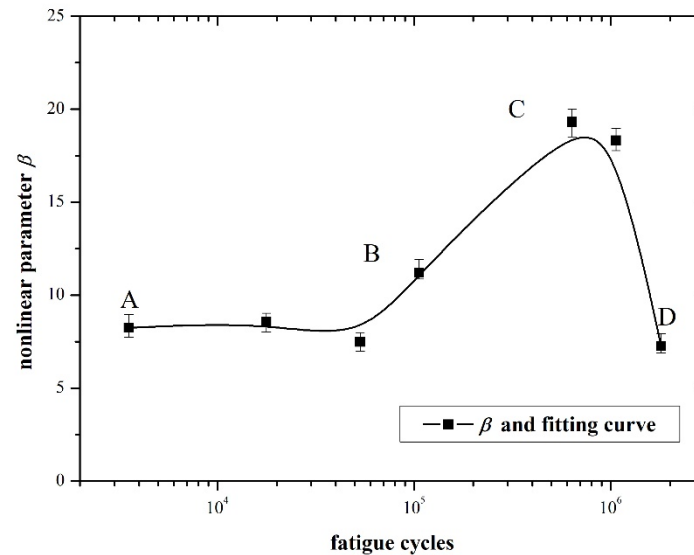


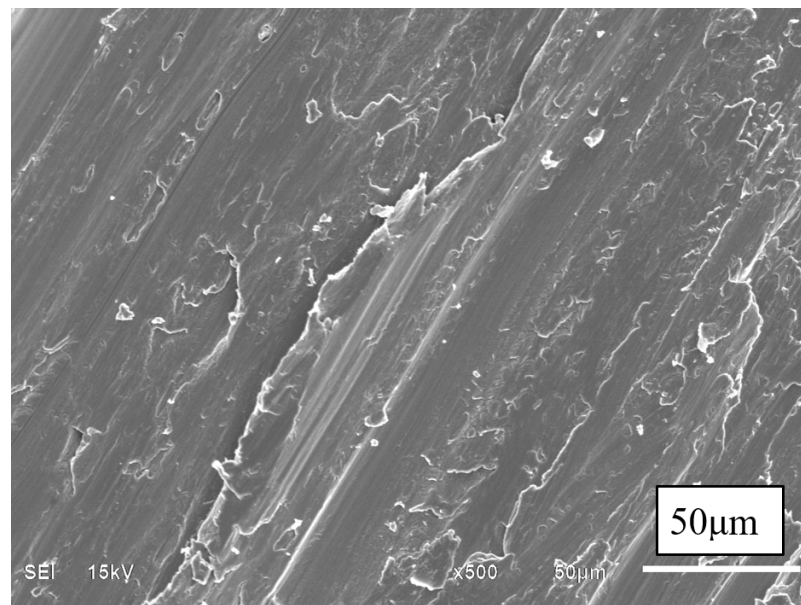
**Figure 7.** Relationship curve between nonlinear coefficient and fatigue cycles of the KMN vibration fatigue specimen. ( $R^2 = 0.93$ ).

From the figure, we can see that the nonlinear coefficient showed a trend of first rising and then falling with the increase in the number of fatigue cycles. At the beginning of fatigue (about before  $5 \times 10^4$  cycles), there were a few micro-defects inside the material. The fatigue damage at this time was mainly a small amount of dislocation slip and microstructure deterioration. These few defects cannot cause significant changes in the second harmonic, so the nonlinear coefficient  $\beta$  remained basically constant. In the early stage of fatigue (before  $10^6$ ), the nonlinear coefficient  $\beta$  increased with the increase in the number of fatigue cycles. The nonlinear coefficient  $\beta$  reached its peak when the micro-cracks started to initiate. In the late stage of the specimen's fatigue life (after  $10^6$ ), the nonlinear coefficient decreased. This shows that there is a corresponding relationship between the nonlinear coefficient  $\beta$  of the material and the fatigue damage. As the number of fatigue cycles increased, the fatigue damage inside the specimen also accumulated. When the ultrasonic wave signal propagated inside the material, the second harmonic wave excited by the sound wave at the damage also increased, and finally the nonlinear coefficient  $\beta$  of the material continued to increase. As the internal fatigue damage degree increased, the appearance of cracks increased the attenuation coefficient of the material, resulting in a decrease in the nonlinear coefficient in the late fatigue life.

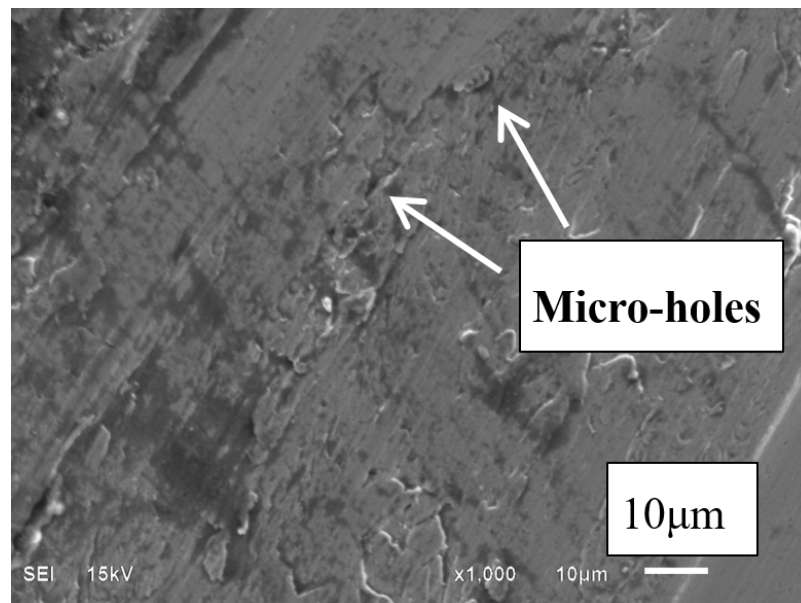
### 3.3. Microscopic Morphology Analysis

In order to further study the relationship between the nonlinear coefficient and the micro-damage inside the material, the stress-concentration zone of the KMN vibration fatigue specimen was dissected and its microscopic appearance was observed. At the narrowest part of the specimen, there was a maximum stress level, and fatigue cracks initiated from this position. It was found that as the number of fatigue cycles increased, the microstructure of the specimen deteriorated relatively, as shown in Figure 8. Figure 8a presents the original specimen, and the material matrix is relatively flat. There were no obvious defects, and the nonlinear coefficient  $\beta$  corresponding to point A in Figure 7 was low. At the beginning of fatigue (about before  $5 \times 10^4$  cycles), there were a few micro-defects inside the material, so the nonlinear coefficient  $\beta$  remained basically constant. As the number of fatigue cycles increased, we can see from Figure 8b that the material had tiny defects such as micro-holes. Corresponding to point B in Figure 7, the

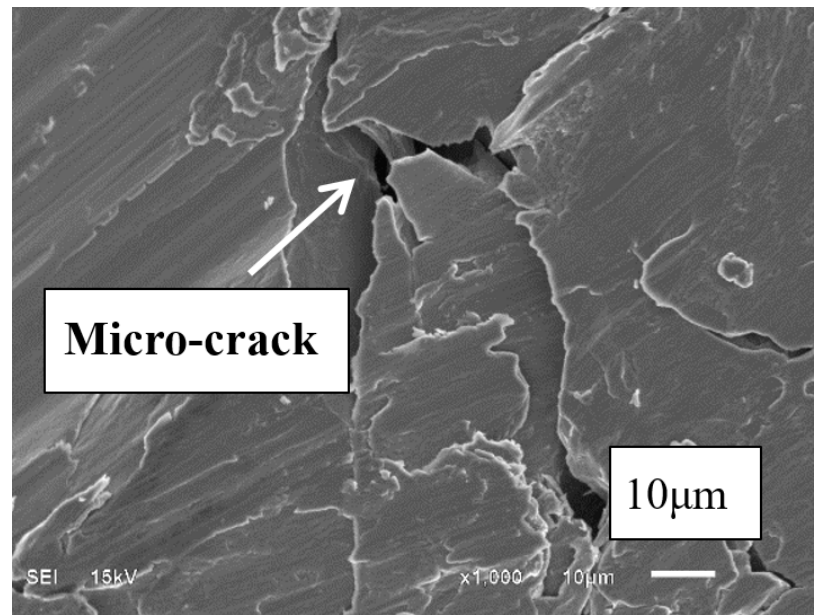
nonlinear coefficient  $\beta$  increased slightly. From Figure 8c, we can see that there were micro cracks in the material matrix. Corresponding to point C in Figure 7, the nonlinear coefficient  $\beta$  increased significantly and reached the peak value. With the further increase in the number of fatigue cycles, the specimen displayed macroscopically large cracks, as shown in Figure 8d. The appearance of cracks increased the attenuation coefficient, resulting in a decrease in the nonlinear coefficient. Corresponding to point D in Figure 7, the nonlinear ultrasonic coefficient  $\beta$  began to decrease. It was proved that there is a corresponding relationship between the material's nonlinear coefficient  $\beta$  and the material's internal damage, and the material's nonlinear coefficient  $\beta$  can be used to characterize the material's fatigue damage.



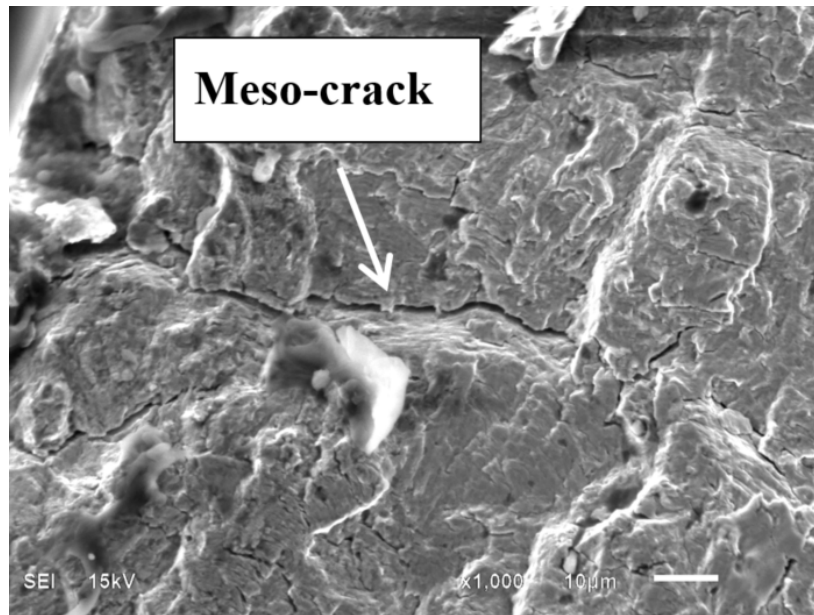
(a)



(b)



(c)



(d)

**Figure 8.** SEM microstructure of KMN vibration fatigue specimen. (a) Point A in Figure 7; (b) point B in Figure 7; (c) point C in Figure 7; (d) point D in Figure 7.

Industrial CT can clearly, accurately, and intuitively display the internal structure, composition, material, and defect status of the detected object in the form of two-dimensional tomographic images or three-dimensional images with no damage to the material. It is the most commonly used nondestructive testing today. Using industrial CT (resolution 0.1667 mm) to perform tomography on the specimens at different fatigue stages, no obvious defects were found [22]. This is because the defects at the early stage of fatigue were too small to be detected by industrial CT. However, the nonlinear coefficient  $\beta$  showed a noticeable change in Figure 7. This proves that nonlinear ultrasonic testing is more sensitive to

small defects and can detect small defects that cannot be found by industrial CT. Therefore, it can be used for the detection of materials at the initial stage of fatigue damage.

### 3.4. $\beta$ - $N$ Curve and Fracture Characteristics of Compressor Blade

We obtained the complete blade from the KMN compressor impeller and processed it into a specimen to keep its surface in service. In addition, we chose a blade specimen to polish the surface as a control specimen. The blade specimens were loaded with different cycles of fatigue, and then the RitecSNAP ultrasonic system was used for nonlinear ultrasonic testing to obtain the relationship curve between the nonlinear ultrasonic coefficient  $\beta$  and the cycle of fatigue, as shown in Figure 9.

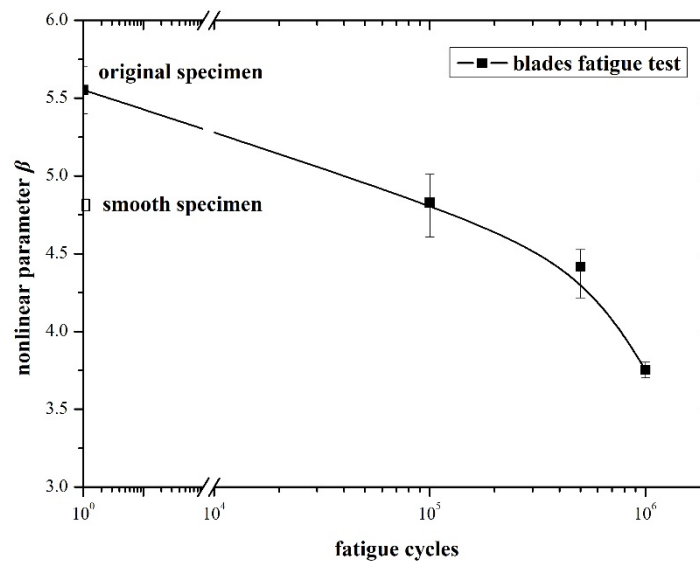


**Figure 9.** Relationship curve between nonlinear coefficient and fatigue cycles of KMN blade fatigue specimen.

It can be seen from Figure 10 that the nonlinear coefficient  $\beta$  of the blade fatigue specimen gradually decreased with the increase in the number of fatigue cycle. This is because the blades of the impeller have been in service for a long time, and defects such as fatigue micro-cracks have been generated inside. The blade has entered the late stage of its fatigue life, that is, the falling stage of the  $\beta$ - $N$  curve. At this time, the micro-cracks inside the specimen cause the attenuation coefficient of the material to increase, and the nonlinear coefficient  $\beta$  decreases with the increase in the number of fatigue cycles. In addition, the original specimen and smooth specimen in Figure 10 were used to study the influence of surface condition on nonlinear coefficient. Because the Lamb wave propagates inside the material, the defects inside the specimen are more important than surface condition. Comparing the original specimen and the smooth specimen, it could be found that the nonlinear coefficient of the smooth specimen was slightly lower than that of the original specimen, but the difference between the two was not much. This is because the nonlinear ultrasonic Lamb wave propagates inside the specimen, and the signal received in the experiment mainly comes from the second harmonics excited by the internal defects of the specimen. Therefore, the measured nonlinear coefficient was more sensitive to the internal defects of the specimen, which shows that the nonlinear ultrasonic detection can be used for the detection of small damage and defects in the initial fatigue stage of the material.

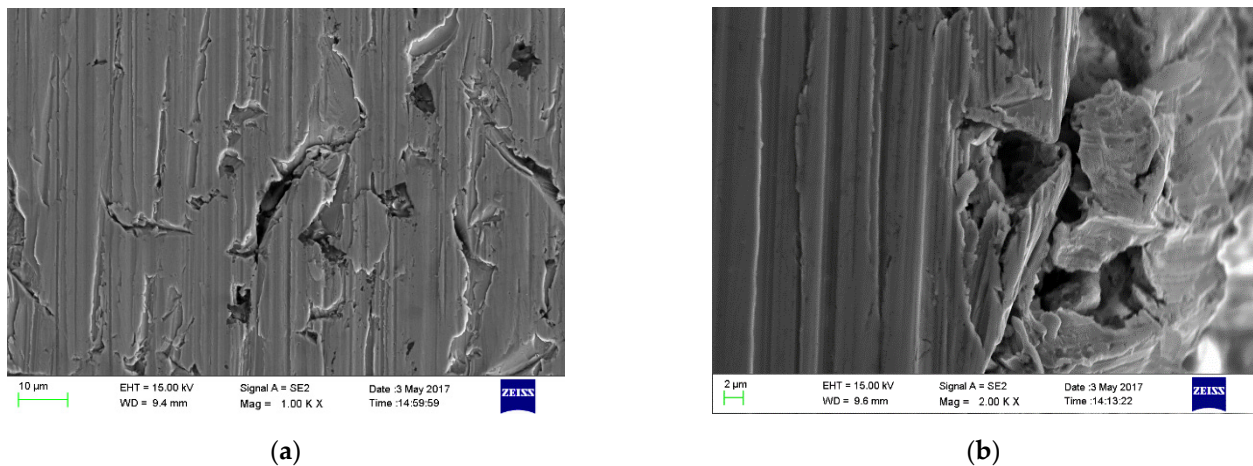


**Figure 10.** SEM Microstructure of KMN blade fatigue specimen. (a) The middle of the cross section; (b) the cross section close to the surface.

The stress-concentration zone, that is, the narrowest part of the specimen, of the fatigue specimen of the KMN blade was dissected, and its microscopic appearance was observed. It was found that there were a large number of microscopic defects such as holes and cracks inside the specimen, which also proved that the blade had entered the late stage of fatigue life at this time, as shown in Figure 10.

#### 4. Discussion

##### 4.1. $\beta$ -a Curve

As the number of fatigue load cycles increases, the microstructure of the specimen will become defective and cracks will form, which will eventually lead to fatigue failure. Combined with the microstructural analysis of the stress-concentration zone of the vibration fatigue specimen, the number and length of fatigue cracks in the 10 standard fields ( $500 \times 500 \mu\text{m}$ ) of view of each specimen were counted, as shown in Table 4. The equivalent crack length refers to the sum of all crack lengths in 10 standard fields [30–33]. Since the received signal of the nonlinear ultrasonic Lamb wave is the sum of the second harmonic generated by all of the defects in the sampling area, it is more reasonable to use the equivalent crack length in the research than the single crack length. From Figure 11, we can see that the number of cracks and the equivalent crack length continued to increase with the increase of fatigue cycles, reflecting the process of continuous crack propagation in the specimen. In particular, when the specimen had large macro-cracks, the number and size of the internal cracks increased significantly.

**Table 4.** Statistics of micro-cracks in the KMN-I vibration fatigue specimens.

Fatigue Cycles	$5 \times 10^4$	$3 \times 10^5$	$5 \times 10^5$	$7 \times 10^5$	$10^6$	$10^7$
Number of cracks	0	1	1	4	5	>50
Crack length/ $\mu\text{m}$	0	8	13	15, 12, 10, 20	8, 12, 14, 30, 15	70, 18, 26 ...
Equivalent crack length/ $\mu\text{m}$	0	8	13	57	79	>600
Standard deviation for crack length	-	-	-	19.49	26.87	-

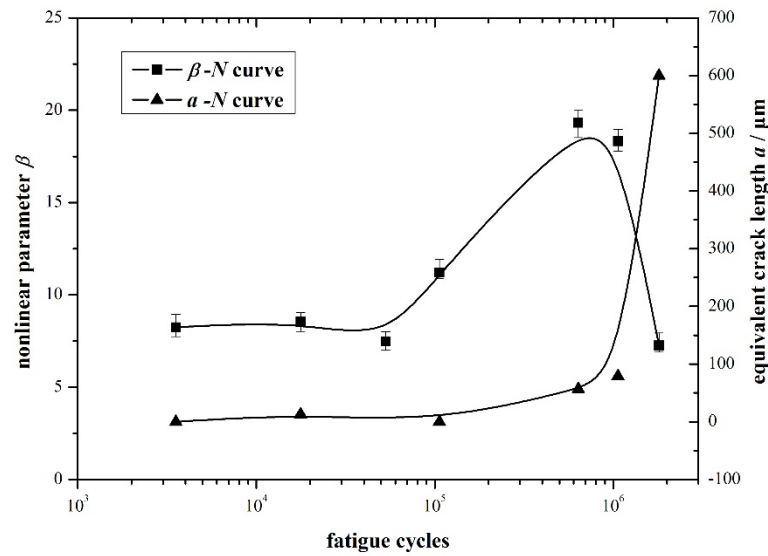


**Figure 11.** Relationship between nonlinear coefficient  $\beta$ , equivalent crack length, and fatigue cycles of the KMN vibration fatigue specimens. ( $R^2 = 0.93$  for  $\beta$ - $N$  curve).

In order to further analyze whether there is a connection between the micro-cracks inside the specimen and the measured nonlinear coefficients, we established the relationship curve between the equivalent crack length of the material and the nonlinear coefficient (i.e., the  $\beta$ - $a$  curve). It can be seen from Figure 12 that, as the length of the crack increased, the nonlinear coefficient of the material also increased, indicating that there is indeed a certain corresponding relationship between the nonlinear coefficient and the propagation of the crack, so we can use the nonlinear coefficient to reflect the propagation process of fatigue cracks inside the material.

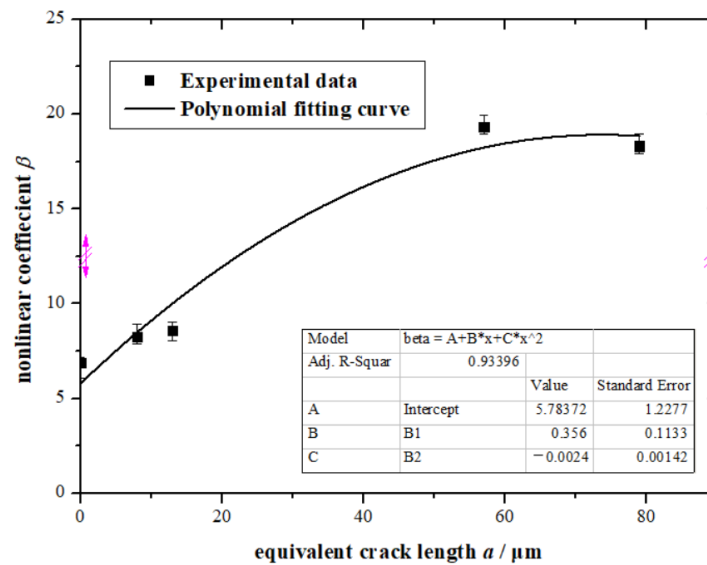


**Figure 12.** Relationship between equivalent crack length and nonlinear coefficient of the KMN vibration fatigue specimens.

On the basis of the KMN vibration fatigue test in this paper, two sets of KMN specimens for the bending fatigue test and tensile-bending fatigue test were added. Their normalized nonlinear coefficients and the equivalent crack length were obtained, and then, the relationship curve between the KMN nonlinear coefficient and the crack growth size was obtained, as shown in Figure 13.

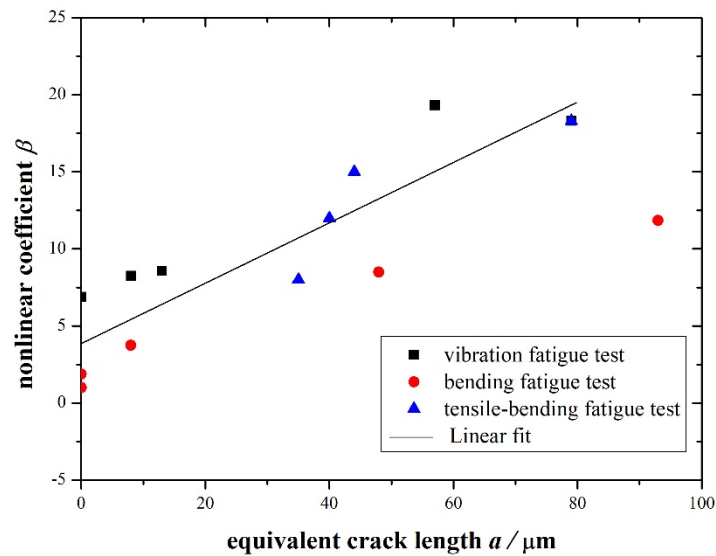


Figure 13. Relationship between nonlinear coefficient and crack propagation size. ( $R^2 = 0.79$ ).

Fitting the data points in the figure, we can establish the empirical formula of the blade material KMN nonlinear coefficient and the crack growth size:

$$\beta = 4.04 + 0.19a \tag{1}$$

Therefore, we can obtain the equivalent crack size of the KMN blade after service through the empirical formula and nonlinear ultrasonic detection. Combined with the KMN very high cycle fatigue life prediction model (Equation (2)) that we derived before [24], the fatigue life of the KMN blade after service can be obtained.

$$N_f = N_i + N_p = \frac{18GW_s}{(\Delta\sigma - \Delta\sigma_{-1})^2\pi(1 - \nu)l} + \frac{a_0^{(1-\frac{n}{2})}}{C\Delta\sigma^n\beta_1^n\pi^{\frac{n}{2}}(\frac{n}{2} - 1)} \tag{2}$$

where  $N_i$  is the initiation life of the crack,  $N_p$  is the propagation life of the crack,  $W_s$  is the specific fracture energy,  $G$  is the shear modulus of the KMN matrix,  $l$  is the semilength of the slip band and  $\nu$  is Poisson’s ratio.  $l$  is about half the grain size ( $10 \mu\text{m}$ ). The specific fracture energy of low carbon steel ( $W_s \approx 3.8 \times 10^5 \text{ N}\cdot\text{m}^{-1}$ ) was used in this study.  $C$  is  $2.0 \times 10^{-11}$  and  $n$  is 2.5 [34].  $\beta_1$  is the geometric constant ( $\beta_1 = 0.5\sqrt{\pi}$ ).

#### 4.2. Fatigue Damage Evaluation Method Based on Nonlinear Ultrasonic Detection

In the previous research, we obtained a very high cycle fatigue  $S-N$  curve and  $\beta-N$  curve of the blade material KMN, both of which reflect the fatigue performance of the material [22–24]. In order to observe the relationship between the two more intuitively, we created a  $\beta-S-N$  three-dimensional model containing the  $S-N$  plane and the  $\beta-N$  plane, as shown in Figure 14. It can be seen from the figure that the  $\beta-N$  curve we studied is the change in the nonlinear coefficient  $\beta$  under the stress of a certain point in the  $S-N$  curve with the increase of fatigue cycles, and the maximum value is the fatigue life corresponding to the stress.

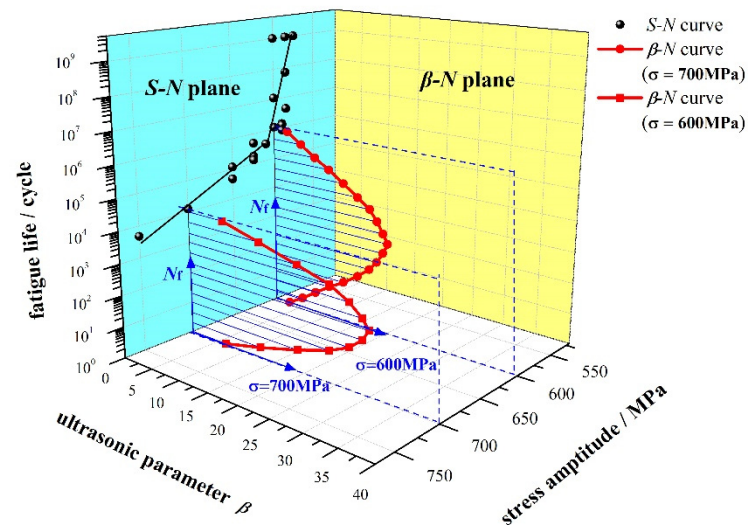


Figure 14. Schematic diagram of the  $\beta$ - $S$ - $N$  three-dimensional model.

Corresponding to any point on the  $S$ - $N$  curve, the fatigue life is  $N_f$ . The nonlinear ultrasonic testing of the material was carried out, and then the  $\beta$ - $N$  curve when the fatigue life is  $N_f$  can be obtained.  $\beta$ - $S$  plane is mainly used to describe the relationship between  $\beta$  and stress. Normally, a larger stress level will result in a higher value of  $\beta$ . The dislocation string model was used to convert the nonlinear ultrasonic  $\beta$ - $N$  curve measured under the calibrated stress [35–38], and the nonlinear ultrasonic  $\beta$ - $N$  curve under arbitrary load can be obtained.

Since the  $\beta$ - $N$  curve of KMN is not monotonous, the measured  $\beta$  value may correspond to two fatigue cycles. In actual operation, we can perform two nonlinear ultrasonic inspections of the blade with an interval of service time. Through the comparison of the two test results, it is judged as to whether the fatigue damage degree of the blade is in the rising phase or the falling phase of the  $\beta$ - $N$  calibration curve at a specific time, and then the fatigue damage degree of the blade in service is determined.

Through the above research and analysis, we can propose an evaluation method for blade fatigue damage based on nonlinear ultrasonic testing. We performed nonlinear ultrasonic testing of the blade in service to obtain the nonlinear coefficient of the blade at a specific time. By comparing the  $\beta$ - $S$ - $N$  three-dimensional model, the fatigue damage degree and fatigue cycle of the blade after service could be obtained so as to determine whether there are micro-cracks inside the blade, and we could formulate the corresponding maintenance and inspection plans to ensure the safe and reliable operation of the centrifugal compressor blade.

## 5. Conclusions

The vibration fatigue test of the blade material KMN under simulated working conditions was carried out. The relationship of the nonlinear coefficient and fatigue damage degree was studied by nonlinear ultrasonic testing. The following conclusions were obtained:

- (1) We obtained the nonlinear coefficient–fatigue cycle curve of the blade material KMN. It was found that the nonlinear coefficient of the material first increased and then decreased with an increase in the number of fatigue cycles.
- (2) The microstructure analysis of the cross section of the specimens was carried out, and the relationship between the expansion of the micro-crack inside the material and the nonlinear coefficient was analyzed. As the number of fatigue cycles increased, the microstructure of the specimen gradually deteriorated and cracks occurred. This proves that nonlinear ultrasonic detection can be used to characterize the micro-cracks in the early fatigue stage of materials. The nonlinear coefficient  $\beta$  of the material can be used to reflect the fatigue damage inside the material.

- (3) Through the statistical analysis of the internal micro-crack size in the early fatigue damage test, the empirical formula of the nonlinear coefficient  $\beta$  and the equivalent crack size was obtained. Combining the  $\beta$ - $N$  curve with the  $S$ - $N$  curve of the blade material KMN under very high cycle fatigue, a  $\beta$ - $S$ - $N$  three-dimensional model was established, and then an evaluation for the initial fatigue damage of the blade fatigue based on nonlinear ultrasonic testing was proposed.

**Author Contributions:** P.W. contributed to formal analysis, and edited the manuscript; W.W. contributed to methodology and performed data curation; S.Z. and B.C. completed the experiment. Z.G. was involved in project administration. All authors have read and agreed to the published version of the manuscript.

**Funding:** This research was funded by National Natural Science Foundation of China (Grant No. 51905484) and Zhejiang Province Public Welfare Technology Application Research Project (Grant No. LGG20E050018).

**Institutional Review Board Statement:** Not applicable.

**Informed Consent Statement:** Not applicable.

**Data Availability Statement:** Not applicable.

**Acknowledgments:** Thanks for the test equipment provided by Shandong University.

**Conflicts of Interest:** The authors declare no conflict of interest.

## References

- Bai, Y.; Guo, T.; Wang, J.; Gao, J.; Gao, K.; Pang, X. Stress-sensitive fatigue crack initiation mechanisms of coated titanium alloy. *Acta Mater.* **2021**, *217*, 117179. [[CrossRef](#)]
- Cantrell, J.H. Substructural organization, dislocation plasticity and harmonic generation in cyclically stressed wavy slip metals. *Proc. R. Soc. A* **2004**, *460*, 757–780. [[CrossRef](#)]
- Ohtani, T. Acoustic damping characterization and microstructure evolution during high-temperature creep of an austenitic stainless steel. *Metall. Mater. Trans. A* **2005**, *36*, 2967–2977. [[CrossRef](#)]
- Herrmann, J.; Kim, J.Y.; Jacobs, L.J.; Qu, J.; Littles, J.W.; Savage, M.F. Assessment of material damage in a nickel-base superalloy using nonlinear Rayleigh surface waves. *J. Appl. Phys.* **2006**, *99*, 124913. [[CrossRef](#)]
- Kim, J.Y.; Jacobs, L.J.; Qu, J.; Littles, J.W. Experimental characterization of fatigue damage in a nickel-base superalloy using nonlinear ultrasonic waves. *J. Acoust. Soc. Am.* **2006**, *120*, 1266–1273. [[CrossRef](#)]
- Yan, B.S.; Wu, B.; Zeng, X.C.; He, C.F. FEM simulation and experimental study of fatigue damage measurement in magnesium using nonlinear ultrasonic. In Proceedings of the 2010 International Conference on Mechanic Automation and Control Engineering, Wuhan, China, 26–28 June 2010.
- Zhou, Z.G.; Liu, S.M. Research, application and development of nonlinear non-destructive testing technology. *Chin. J. Mech. Eng.* **2011**, *47*, 2–11. [[CrossRef](#)]
- Nagy, P.B. Fatigue damage assessment by nonlinear ultrasonic materials characterization. *Ultrasonics* **1998**, *36*, 375–381. [[CrossRef](#)]
- Jhang, K.Y.; Kim, K.C. Evaluation of material degradation using nonlinear acoustic effect. *Ultrasonics* **1999**, *37*, 39–44. [[CrossRef](#)]
- Kawashima, K.; Ito, T.; Nagata, Y. Detection and Imaging of Nonmetallic Inclusions in Continuously Cast Steel Plates by Higher Harmonics. *Jpn. J. Appl. Phys.* **2010**, *49*, 07HC11. [[CrossRef](#)]
- Viswanath, A.; Rao, B.P.C.; Mahadevan, S.; Parameswaran, P.; Jayakumar, T.; Baldev, R. Nondestructive assessment of tensile properties of cold worked AISI type 304 stainless steel using nonlinear ultrasonic technique. *J. Mater. Process. Technol.* **2011**, *mbxemp211*, 538–544. [[CrossRef](#)]
- Cremer, M.; Zimmermann, M.; Christ, H.J. In-Situ Characterization of the Damage Evolution of Welded Aluminum Alloy Joints during Very High Cycle Fatigue (VHCF) with Nonlinear Ultrasonic Technique. In *Supplemental Proceedings: Materials Properties, Characterization, and Modeling*; John Wiley & Sons, Inc.: Hoboken, NJ, USA, 2012; Volume 2, pp. 839–846.
- Li, W.; Cui, H.; Wen, W.; Su, X.; Engler-Pinto, C.C., Jr. In situ nonlinear ultrasonic for very high cycle fatigue damage characterization of a cast aluminum alloy. *Mater. Sci. Eng. A* **2015**, *645*, 248–254. [[CrossRef](#)]
- Yan, H.J. Research on Nonlinear Ultrasonic Testing Method for Fatigue Damage of Metal Components. Ph.D. Thesis, Beijing Institute of Technology, Beijing, China, 2015.
- Yan, H.J.; Xu, C.G.; Xiao, D.G. Research on Nonlinear Ultrasonic Characteristics of Metallic Material Tensile Stress. *J. Mech. Eng.* **2016**, *52*, 22–29. [[CrossRef](#)]
- Feng, W. Multi-Point Rapid Non-Linear Ultrasonic Testing of Fatigue Damage of Aluminum Alloy. Ph.D. Thesis, Harbin Institute of Technology, Harbin, China, 2015.

17. Li, H.Y.; Shi, Y.H.; Wang, Z.B. Using Nonlinear Surface Waves to Evaluate Material Fatigue Damage. *Acoust. Technol.* **2019**, *38*, 296–300.
18. Gao, L.; Chen, Z.H.; Li, C.G. Non-linear guided wave detection of fatigue damage of aluminum alloy plates. *Nondestruct. Test.* **2020**, *42*, 61–65.
19. Wang, H.F. Research on Metal Fatigue Damage Detection and Location Based on Nonlinear Ultrasound. Ph.D. Thesis, Tianjin University, Tianjin, China, 2017.
20. Zhang, F.Y. Research on Material Damage Detection Based on Nonlinear Ultrasound. Ph.D. Thesis, Zhengzhou University, Zhengzhou, China, 2019.
21. Bian, L.Y. Research on Plate Damage Identification and Location Based on Ultrasonic Lamb Wave. Ph.D. Thesis, Dalian University of Technology, Dalian, China, 2019.
22. Wang, P.F.; Wang, W.Q.; Li, J.F. Research on Fatigue Damage of Compressor Blade Steel KMN-I Using Nonlinear Ultrasonic Testing. *Shock. Vib.* **2017**, *2017*, 4568460. [[CrossRef](#)]
23. Wang, P.F.; Wang, W.Q.; Zhang, M.; Zhou, Q.W.; Gao, Z.L. Effects of Specimen Size and Welded Joints on the Very High Cycle Fatigue Properties of Compressor Blade Steel KMN-I. *Coatings* **2021**, *11*, 1244. [[CrossRef](#)]
24. Wang, P.F.; Wang, W.Q.; Li, J.F. Fatigue behavior and mechanism of KMN in a very high cycle regime. *Mater. Test.* **2018**, *60*, 55–60. [[CrossRef](#)]
25. Wang, P.F. Research on High/Very High Cycle Fatigue Mechanism and Residual Life Estimation Method of KMN Steel. Ph.D. Thesis, Shandong University, Jinan, China, 2018.
26. Xiang, Y.X. Research on Nonlinear Ultrasonic Guided Wave Evaluation Method for Early Damage of High Temperature Components. Ph.D. Thesis, East China University of Science and Technology, Shanghai, China, 2011.
27. Matlack, K.H.; Kim, J.Y.; Jacobs, L.J.; Qu, J. Review of Second Harmonic Generation Measurement Techniques for Material State Determination in Metals. *J. Nondestruct. Eval.* **2015**, *34*, 273. [[CrossRef](#)]
28. Croxford, A.J.; Wilcox, P.D.; Drinkwater, B.W.; Nagy, P.B. The use of non-collinear mixing for nonlinear ultrasonic detection of plasticity and fatigue. *J. Acoust. Soc. Am.* **2009**, *126*, 117–122. [[CrossRef](#)]
29. Cantrell, J.H.; Yost, W.T. Nonlinear ultrasonic characterization of fatigue microstructures. *Int. J. Fatigue* **2001**, *23*, 487–490. [[CrossRef](#)]
30. Moura, D.M.; Morais, A.D. Equivalent crack based analyses of ENF and ELS tests. *Eng. Fract. Mech.* **2008**, *75*, 2584–2596. [[CrossRef](#)]
31. Mikkola, E.; Murakami, Y.; Marquis, G. Equivalent crack approach for fatigue life assessment of welded joints. *Eng. Fract. Mech.* **2015**, *149*, 144–155. [[CrossRef](#)]
32. Huang, Y.; Ye, X.; Hu, B.; Chen, L. Equivalent crack size model for pre-corrosion fatigue life prediction of aluminum alloy 7075-T6. *Int. J. Fatigue* **2016**, *88*, 217–226. [[CrossRef](#)]
33. Luo, Y.H.; Wu, X.; Ding, Z.N.; Feng, X.H. Fatigue life prediction of box girder of bridge based on equivalent crack approach. *J. Mech. Strength* **2018**, *40*, 200–204.
34. Wang, Q.Y.; Berard, J.Y.; Rathery, S.; Bathias, C. Technical note High-cycle fatigue crack initiation and propagation behaviour of high-strength spring steel wires. *Fatigue Fract. Eng. Mater. Struct.* **1999**, *22*, 673–677. [[CrossRef](#)]
35. Hikata, A.; Chick, B.B.; Elbaum, C. Dislocation contribution to the second harmonic generation of ultrasonic waves. *J. Appl. Phys.* **1965**, *36*, 229–236. [[CrossRef](#)]
36. Hikata, A.; Elbaum, C. Generation of ultrasonic second and third harmonics due to dislocations. I. *Phys. Rev.* **1966**, *144*, 469. [[CrossRef](#)]
37. Hikata, A.; Sewell, F.A., Jr.; Elbaum, C. Generation of ultrasonic second and third harmonics due to dislocations. II. *Phys. Rev.* **1966**, *151*, 442. [[CrossRef](#)]
38. Hull, D.; Bacon, D.J. *Introduction to Dislocations*; Butterworth-Heinemann: Oxford, UK, 2001.